Semiconductor Physics, Quantum Electronics & Optoelectronics, 2016. V. 19, N 4. P. 343-351.
doi: https://doi.org/10.15407/spqeo19.04.343

PACS 61.05.cp, 61.72.Hh, 78.55.Hx

$SrTiO_3:Eu^{3+}$ phosphors prepared by sol-gel synthesis: Structural characterization, magnetic properties and luminescence spectroscopy study

A.S. Pusenkova, O.N. Marchylo, L.V. Zavyalova, I.S. Golovina, S.V. Svechnikov, B.A. Snopok
V. Lashkaryov Institute of Semiconductor Physics, NAS of Ukraine
41, prospect Nauky, 03680 Kyiv, Ukraine

Abstract. We report the results of the comprehensive study of the structural, magnetic and optical properties of $SrTiO_3$ perovskite doped with Eu^{3+} ions. Polycrystalline powders were obtained by sol-gel process including high-temperature annealing at 1300 °C. The structural analysis showed that material is composed of several phases with dominant $SrTiO_3$ and considerable quantity of titanium dioxide (rutile, 10…20%). Both the amount of Eu and ratio of Eu:Sr in the final product are considerably smaller as compared to the original solutions for synthesis. The elemental analysis reveals europium only in the phase of $EuSrTi_2O_7$ compound for equimolar ratio of Eu and Sr during the synthesis. The EPR analysis reports deficiency of Eu^{2+} in the samples under investigations. $SrTiO_3:Eu^{3+}$ powders demonstrate weak photoluminescence, which intensity grows up with increasing the concentration of Eu and reaches its maximum at c.a. 8 mol.% of Eu in the original solutions. Addition of Al increases the intensity of photoluminescence (c.a. 2.2 for 10 mol.%). Emission spectra are typical for Eu^{3+} occupied sites with high symmetric environment (dominant $^5D_0 \rightarrow {}^7F_1$ transition) with relatively low distortion (both $^5D_0 \rightarrow {}^7F_2$ and $^5D_0 \rightarrow {}^7F_4$ as well present, but with a lower intensity) of coordination polyhedron. Low solid-solubility limit of Eu^{3+} in perovskite matrix (less than 1 mol.%), peculiarities of optical spectra, effect of Al, production/annealing temperature dependence *etc.* have suggested that structural effects are dominating in functional, in particular, optical properties of $SrTiO_3:Eu^{3+}$ phosphors.

Keywords: sol-gel synthesis, photoluminescence, $SrTiO_3:Eu^{3+}$ phosphors.

Manuscript received 07.06.16; revised version received 18.08.16; accepted for publication 16.11.16; published online 05.12.16.

1. Introduction

Inorganic and especially ceramic phosphors are among the promising materials for the next generation of solid-state lighting, such as device indicators, backlights, automobile headlights and conventional household illumination. In particular, rare earth elements doped phosphors have attracted significant attention due to their potential application for various kinds of fluorescent emitters (including those with conversion of UV radiation based on photon cutting), X-ray detectors and multi-color visualization tools. Researches in this area stimulate progress in using the phosphors in vacuum ultraviolet radiation excited plasma display panels, mercury-free fluorescent lamps and in the development of efficient solar cells [1-3].

Semiconductor Physics, Quantum Electronics & Optoelectronics, 2016. V. 19, N 4. P. 343-351.
doi: https://doi.org/10.15407/spqeo19.04.343

Among others, perovskites with accommodated Eu ions are promising materials due to strong interaction between the structural order parameter, polarization and magnetization, which leads to their application in the field of multiferroic nano-systems. Indeed, the matrix based on the $SrTiO_3$ structure has attracted great interest due to its special structure features, excellent physical and chemical stability. Instead of the fact that this interest is unrelaxing more than half century, many questions are still open and the new ones continually arise. For example, nanosized materials based on $Eu_xSr_{1-x}TiO_3$ solid solution can exhibit not only all the interesting structural and polar mode interactions of individual $EuTiO_3$ and $SrTiO_3$ films but also new phenomena and properties [4-9]. There has been one experimental study on the structural antiferrodistortive and other physical properties of bulk solid solution $Eu_xSr_{1-x}TiO_3$ [10]. Theoretically, possible multiferroic properties of $Eu_xSr_{1-x}TiO_3$ nanotubes and nanowires [11] have been predicted using the Landau−Ginzburg−Devonshire theory. The vector nature of the antiferrodistortive order parameter can strongly influence the phase stability, twin domain structure, polar and pyroelectric properties of quantum paraelectrics [12] at interfaces [13], or entire thin films [14] of $SrTiO_3$ and $Eu_xSr_{1-x}TiO_3$ [15] (Fig. 1). Hence, the study of the optical and electro-physical properties, long-range structural, magnetic and polar ordering as well as the phase diagrams of $Eu_xSr_{1-x}TiO_3$ is an important problem for fundamental science and promising for advanced application. To achieve that, it is necessary to design the synthetic protocols that make it possible to produce $Eu_xSr_{1-x}TiO_3$ structures with a wide range of the doped europium concentration x inside the perovskite matrix.

Among other rare earth ions, europium is a special element as dopant, because it exhibits not only the property of valence fluctuation (i.e., the valence state may be divalent or trivalent), but the luminescent of Eu^{3+} doped materials are greatly influenced by the matrix as well (the so-called spectroscopic probe). Indeed, the short overview of the emission properties of europium-doped materials clearly confirms this statement – luminescence of the accommodated Eu^{3+} ions strongly depends on both spatial distribution and nature of coordinated ligands [16-21]. So, the difference in optical properties of supposedly the same $SrTiO_3$:Eu^{3+} product obtained by different synthetic procedure clearly indicates the differences of the local environment of emitting ions [16, 22-26]. One of the possible reasons for that is the fact that the most of these materials obtained using the solid phase synthesis, which is peculiar to have spatial heterogeneity in the final material with different phases. Modern tendencies suggest the need for development of liquid-phase techniques, which have the advantage of uniform distribution of components and dopant materials [27-29]. In accord with the mentioned above, the aim of this work is development of technological procedure for production of $SrTiO_3$ with accommodated Eu ions by liquid-phase sol-gel method and detailed characterization of the product concerning the real amount and local surrounding of the europium ions within the perovskite matrix.

2. Structure and morphology of Eu^{3+} doped $SrTiO_3$

$SrTiO_3$:Eu^{3+} powders were prepared as described in [27] using strontium chloride $SrCl_2$ (99.99), europium chloride, $EuCl_3$ (99.9) and titanium tetra-isopropoxide, $Ti(O\text{-}i\text{-}C_3H_7)_4$ (99.999). All reagents were received from KOJUNDO CHEMICAL LABORATORY CO., LTD (Japan) and used without any other additional treatment. The obtained dried gel was calcinated at high temperature for crystallization of final material. The annealing temperature was 1300 °C, annealing time: 5 or 7 hours. The polycrystalline powders were examined to determine their structures as well as phase and elemental compositions. The crystalline structures of the prepared

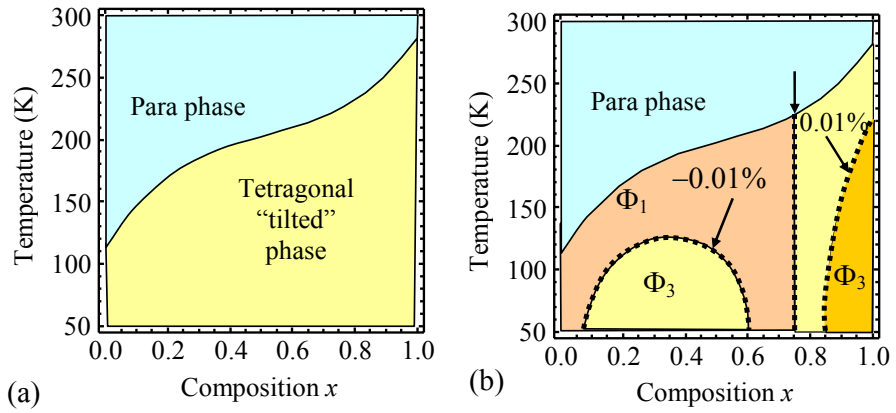

Fig. 1. Temperature-composition phase diagrams of $Eu_xSr_{1-x}TiO_3$ bulk (*a*) and thin films (*b*). Plot (*b*) is calculated for the matched substrate corresponding to zero misfit $u_m = 0$ (vertical boundary Φ_1/Φ_3), $u_m^* = -0.01\%$ (left Φ_3 region), $u_m^* = +0.01\%$ (right Φ_3 region). Designations represent the nonzero components of order parameter – oxygen tilt component Φ_i in a given phase. The abbreviation "para" stands for the paraelectric non-ferrodistortive phase. (Adapted from Ref. [15].)

Semiconductor Physics, Quantum Electronics & Optoelectronics, 2016. V. 19, N 4. P. 343-351.
doi: https://doi.org/10.15407/spqeo19.04.343

Table. Content of elements and separate phases in accord with the data of different analytical methods as a function of the Eu content.

Content of Eu in the initial material, mol.%	t_{ann}, hour	XRD			Elemental analysis			Magnetic resonance	
								Peak signal I_{pp}, rel. un.	
		Eu, wt.%	$SrTiO_3$, wt.%	TiO_2, wt.%	Ti, wt.%	Sr, wt.%	Eu, wt.%	FMR signal with H_{res} = 800 Oe	EPR signal with H_{res} = 3360 Oe
0	5	–	78.4	21.5	59.5	38.5	–	879	150
0	7	–	75.6	24.4	–	–	–	–	–
8	5	–	79.8	20.2	–	–	–	430	180
50	5	30.2 – $EuSrTi_2O_7$	60.4	9.4	52.6	17.1	28.8	260	101

powders were investigated with X-ray diffraction (XRD) on a DRON-3M X-ray diffraction apparatus with Cu K_α radiation (λ = 1.542 Å) as the incident one. The elemental analysis was performed using the X-ray fluorescence spectrometer X "Unique II" (Philips).

Fig. 2 shows the X-ray diffraction patterns for the $SrTiO_3$:Eu^{3+} phosphor with equimolar Eu:Sr ratio in initial solutions. The presented data shows that this material is a polycrystalline powder consisting of several phases: $SrTiO_3$ is the dominating one with an appreciable content of titanium oxide phase (rutile); additional phase is $EuSrTi_2O_7$, which is present only at high content of Eu in initial solutions, despite the fact that the ratio of Eu and Sr in the initial solution was 1:1. If the concentration of europium was less than 8%, Eu compound in crystalline state has not been detected; at the same time, the part of rutile increases up to 20…25%.

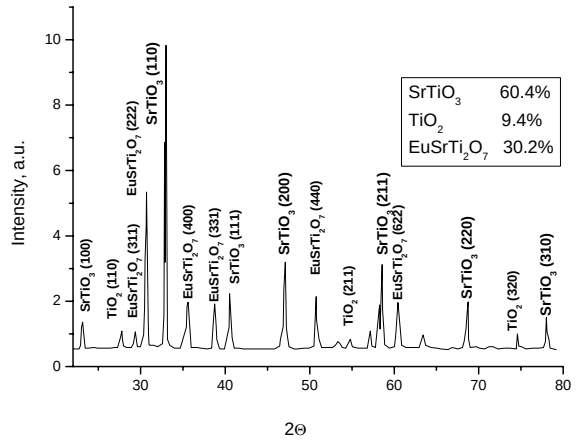

Fig. 2. X-ray spectrum of the sample prepared with the ratio of Sr and Eu in the initial solution as 1:1.

The overview of the results presented in the Table allows to assume that, under the given process conditions, formation of $SrTiO_3$ is energetically more favorable and accommodation of europium occurs only in the case of its "excess" during the synthesis.

It is interesting to highlight that pure $SrTiO_3$ contains a large amount of TiO_2 (20…25%, Table) in the crystalline modification of rutile. Increasing the annealing time does not reduce the amount of TiO_2 in the sample whilst addition of Eu decreases. Moreover, in line with elemental analysis Ti is the predominant component of the powder. One of the possible explanations is as follows. We used the strontium chloride as the initial reagent. Owing to its relatively low boiling temperature, Sr partly evaporated during the annealing process resulting in Ti excess. Redundant Ti precipitated as TiO_2 [30].

As can be seen from the data, as the concentration of europium in the initial solution increases, the proportion of rutile in the final powder reduces. So, addition of Eu diminishes formation of titanium dioxide. Keeping in mind that the amount of europium in the phosphors under consideration is less than the limit of detection, it is reasonable to suggest that the initially formed structures containing both europium and Ti destroyed during annealing at high temperature. As a result, pure perovskite matrix with high temperature stability dominates in this powder. And only in the case of essential "excess" of Eu in the original solutions, a reasonable amount of europium-containing material can be detected simultaneously with relatively low impact of TiO_2.

3. Magnetic properties

Magnetic properties of polycrystalline phosphors were investigated using the EPR method with Radiopan SE/X 2544 X-band radio-spectrometer. Results of the

magnetic properties study of the samples with different Eu-content in the initial materials are shown in Fig. 4 and Table in the form of magnetic resonance spectra. The measurements were performed at room temperature with the frequency 9.386 GHz. The test powder was placed into a silica ampoule. The spectra were normalized to the weight of the samples, which allowed to compare the signals from different samples accurately.

The spectra of all samples are identical and consist of three lines, *A*, *M* and *B*. However, the line A in the range of magnetic field 1500 Oe – signal from Fe^{3+}-ions, located in the glass ampoules, into which the investigated powders were placed. Thus, the samples show two proper signals, *M* and *B*. The resonant magnetic field (H_{res}) and width (ΔH) for each of those signals remain constant from sample to sample. Only their peak intensity (I_{pp}) varies.

The signal *M* of the sample placed in a weak magnetic field H_{res} = 800 Oe is very wide: ΔH = 1600…1700 Oe. Because of the H_{res} low values and a large width, *M* signal is not fully registered. These signals often have a ferromagnetic origin [31]. Obviously, this signal is provided by an uncontrolled magnetic impurity located in the initial reagents that were used in the strontium titanate synthesis. Under doping, the peak intensity of *M* signal decreases, and the line becomes very weak in the sample doped with 50% $EuCl_3$. Possibly, the signal *M* corresponds to the α-Fe phase. Thus, in [32] the authors investigated the FMR signal of α-Fe phase formed after annealing the amorphous alloy $Fe_{90}Zr_7B_3$. This signal has characteristics similar to the characteristics of the signal *M*. It should be noted that the signal M has a line shape of the resonant absorption derivative and is not a reflection of the initial magnetization processes, which are sometimes observed in the FMR spectra of magnetic compounds (called DARMA peaks [33]).

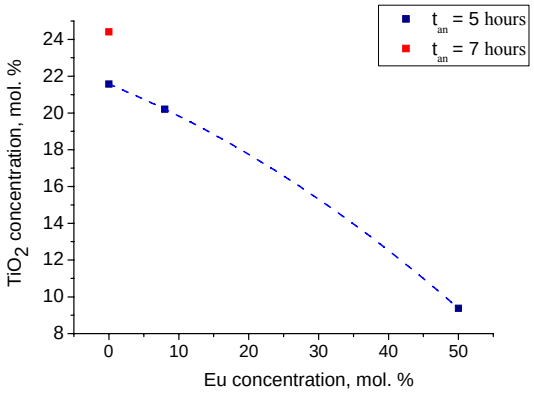

Fig. 3. Content of the oxide phase TiO_2 in the obtained powders $SrTiO_3$:Eu depending on the Eu concentration.

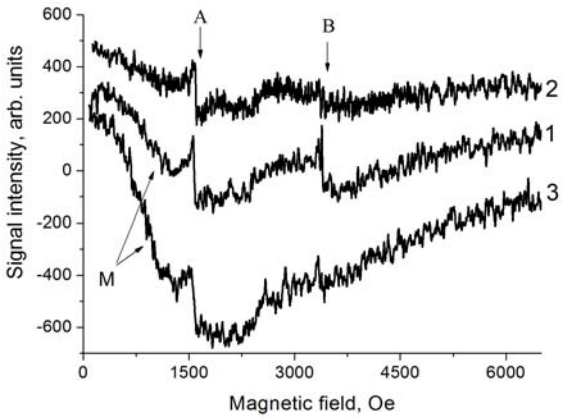

Fig. 4. EPR spectra of the samples comprising in the starting materials 8% $EuCl_3$ (spectrum 1), 50% $EuCl_3$ (spectrum 2) and control sample containing no $EuCl_3$ (spectrum 3).

The narrow signal *B* at H_{res} = 3360 Oe can correspond to both extrinsic and intrinsic defects. The former include, for example Fe^{3+}-ions, randomly included in the material during the synthesis and forming the paramagnetic centers, in the structure of which the oxygen vacancy V(O) is present. This signal from paramagnetic centers Fe^{3+}-V(O) was observed in $KTaO_3$ [34, 35] and $SrTiO_3$ [36]. Defects of internal origin in the investigated powders are, for example, centers of O^- and O^{2-}. EPR signals from these centers were observed in $SrTiO_3$ [37], and in TiO_2 [38]. As it is obvious from Fig. 4, the signal *B* has the lowest intensity in a sample doped with 50% $EuCl_3$. According to the data of X-ray and EPR, listed in Table, $SrTiO_3$ phase amount correlates with the intensity of the signal from sample to sample. From this comparison, it can be assumed that the signal *B* corresponds to the paramagnetic centers formed precisely in this phase. The exact determination of the signal's origin requires a separate investigation and is beyond the scope of this work.

Unlike $Eu_xSr_{1-x}TiO_3$ solid solutions described in [2], the doped samples obtained in this study not exhibit long-range magnetic order resulting from the exchange interaction between the Eu^{2+}-ions. This is quite natural, since according to the X-ray data the sample doped with 8% $EuCl_3$ does not contain europium, and in the sample doped with 50% $EuCl_3$, $EuSrTi_2O_7$ phase is formed. It should be noted that according to [5], as a result of the exchange interaction between Eu^{2+} ions, the low-temperature phase in $Eu_xSr_{1-x}TiO_3$ solid solutions is antiferromagnetic, but the long-range magnetic ordering is realized only in the compositions with $x > 0.25$. This is critical concentration, below which the crossover occurs in the properties of the $Eu_xSr_{1-x}TiO_3$ solutions. Despite the fact that the content of europium in the sample doped with 50% $EuCl_3$ is 28.8% (see Table), all Eu is in the phase of $EuSrTi_2O_7$.

Thus, the EPR signal from the Eu^{2+} ions in our samples was not observed. The result is not so unexpected, keeping in mind that for production of Eu^{2+} containing phosphors usually used is annealing Eu^{3+} phosphors at high temperature (*e.g.*, 1100 °C) in a reductive atmosphere (a mixture of H_2 and N_2 *etc.*) for several hours [39]. Application of the Eu^{2+} compound during the synthesis is not reasonable, since in solutions Eu^{2+} ions are quickly oxidized up to Eu^{3+} [40].

4. Photoluminescent properties of $SrTiO_3$:Eu^{3+} phosphors

The optical properties of crystalline phosphors $SrTiO_3$:Eu^{3+} were investigated for samples annealed at the temperature 1300 °C for 5 hours. The luminescence spectra were recorded using photo-multianalyzer Hamamatsu PMA-12 (Japan) at room temperature. The excitation source was He-Cd laser with the wavelength λ = 325 nm. The concentration of europium in initial solutions during fabrication varied within the range 0.1 to 10.0 mol.%. Fig. 5 demonstrates typical photo-luminescence of $SrTiO_3$: Eu^{3+} samples (0.2 mol.%).

Pure strontium titanate displays a broad spectrum of luminescence in the visible region without any specific bands. This emission spectrum is similar for many perovskite crystals, associated with the presence of imperfections or defects and is typical for materials with localized exciton excitations. For the temperature range more than c.a. 1100 °C, this band usually disappears. Thus, mixed ionic-covalent bonding properties of the $SrTiO_3$ perovskite matrix with a unique electronic structure can be efficiently used to investigate the optical behavior of accommodated ions with their proper emission spectrum. The latter opens the ways to finely tune and adjust properties of $SrTiO_3$ material due to cation substitution.

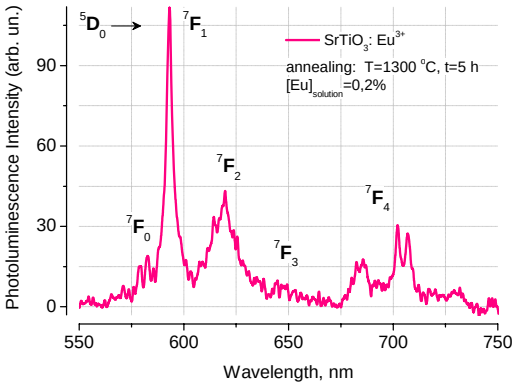

Fig. 5. Crystalline phosphor $SrTiO_3$:Eu photoluminescence spectrum (concentration of Eu is equal to 0.2 mol.%).

Therefore, the presence of Eu^{3+} in the $SrTiO_3$ host results in photoluminescence properties specific for europium ions. Fig. 5 presents the emission spectrum of the Eu^{3+}-doped $SrTiO_3$ powder, excited at 325 nm. The line positions are in good agreement with the energy levels for Eu^{3+} transitions arising from their 4f electrons and described in Ref. [16]. The emission spectrum shows the typical emissions of Eu^{3+} ions occupying the range 500…800 nm; the luminescence peaks can be assigned to the $^5D_0 \rightarrow {}^7F_J$ (J = 0, 1, 2, 3, 4) transitions. The $^5D_0 \rightarrow {}^7F_1$ transition near 593 nm dominates the spectrum and is more intense than the other ones. Furthermore, the $^5D_0 \rightarrow {}^7F_2$ and $^5D_0 \rightarrow {}^7F_4$ transitions are easy detectable and located within 610…630 and 680…710 nm ranges, correspondingly. Similar spectra of the Eu^{3+}-doped $SrTiO_3$ powder were observed F. Fujishiro for the material obtained by the sol–gel based Pechini technique [41], C.R. García *et al.* – prepared by pressure-assisted combustion synthesis with powder post-annealing at 1200 °C [22] and L. Dong *et al*. in $Sr_xBa_{1-x}TiO_3$:Eu^{3+} phosphors synthesized using the high temperature solid-phase method with calcination at 1100 °C, excited with 466 nm [23]. However, at the same time photoluminescence of europium-doped strontium titanate prepared at lower temperature (microwave hydrothermal method at 140 °C [42], in a molten NaCl flux at 950 °C and dehydrated at 120 °C, excitation 488 nm [26], by the sol-gel process with annealing at 750 °C, excitation 460 nm, 77 K) [24]) demonstrate the dominant band around 620 nm that corresponds to the $^5D_0 \rightarrow {}^7F_2$ transition with a low intensity of the $^5D_0 \rightarrow {}^7F_1$ band.

The $^5D_0 \rightarrow {}^7F_1$ transition is the most intense one in the spectra of solids with the centrosymmetric crystal structure [16, 43]. It well correlates with experimental results, if we assume that Eu^{3+} enters the centrosymmetric Sr^{2+} site within the cubic perovskite structure of $SrTiO_3$ [41]. The intensity of this transition is often considered to be constant, since the intensity of a magnetic dipole transition is largely independent of the environment of the Eu^{3+} ion [16]. Moreover, the $^5D_0 \rightarrow {}^7F_1$ transition directly reflects the crystal-field splitting of the $^7F_1$ level. Fig. 5 demonstrates that the $^7F_1$ level is not split, so, europium ions are mainly in highly symmetric environment. However, negligible crystal-field splittings may be a consequence of a high coordination number possible in perovskite matrix (probably, ion is twelve-coordinated): a large number of coordinating atoms distributed fairly evenly around the central metal ion tends to produce approximately spherical field, with small effective asymmetry [16].

The intensity of $^5D_0 \rightarrow {}^7F_2$ transition is essentially smaller in respect to the $^5D_0 \rightarrow {}^7F_1$ band, but still relatively high. Keeping in mind that the intensity of this so-called "hypersensitive transition" is influenced by the local symmetry of the Eu^{3+} ion and the nature of the ligands, it's reasonable to conclude that some distortion can be attributed to local ion surrounding. The reasoning

is that the $^5D_0 \rightarrow {}^7F_2$ is strictly forbidden for the Eu^{3+} ion at the site with a center of symmetry, so that the stronger the distortion of the site from a highly symmetric coordination polyhedron, the more intense the $^5D_0 \rightarrow {}^7F_2$ transition will become [16]. Taking into account that the intensity of the $^5D_0 \rightarrow {}^7F_4$ transition is also easy detectable, it is very likely that high symmetry of coordination polyhedron is partly distorted near the Eu^{3+} ion. It is well known that the substitution of divalent ions by trivalent ions produces distortion of the site symmetry; so, if the Eu^{3+} surely enters into the Sr^{2+} sites, this in turn promotes the $^5D_0 \rightarrow {}^7F_2$ transition. Contrary to that, the higher intensity of the $^5D_0 \rightarrow {}^7F_2$ transition as compared with the $^5D_0 \rightarrow {}^7F_1$ one observed in the luminescence spectrum of $SrTiO_3$:Eu^{3+} materials in Refs. [26, 24, 42] may be attributed to low symmetry of Eu^{3+}, if suggesting strong distortion around the Eu^{3+} sites. This different behavior can be explained, if the europium enters not only into Sr^{2+} (as in the latter case) but into Ti^{4+} sites at the same time, too, as reported by Jiang *et al*. [44]. This mechanism can lead to a low degree of distortions and, probably, can be realized only at high temperatures (more than 1000 °C). This suggestion well correlates with the difference in emission spectra discussed above.

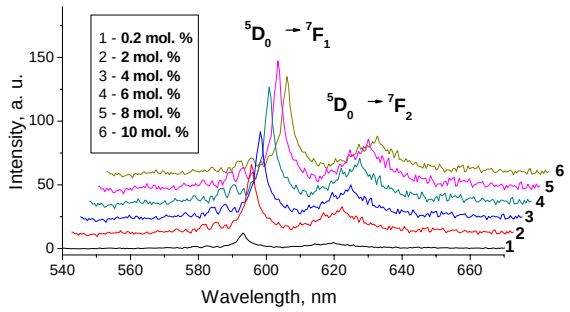

a)

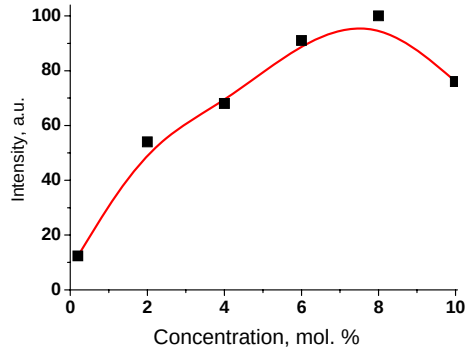

b)

Fig. 6. PL spectrum of $SrTiO_3$:Eu^{3+} at various concentrations of Eu (a) and dependence of the PL intensity at λ = 593 nm on the concentration of europium (b).

Europium free $SrTiO_3$ does not show luminescence. With increasing the concentration of Eu^{3+}, the intensity of the bands increases without changing the overall spectrum shape (Fig. 6). Indeed, this figure shows that with increasing the Eu concentration within the range 0.2 to 10 mol.% all peaks in the wavelength range λ = 580…710 nm remain the same. A similar dependence was obtained in [23], the optimum doping concentration 5% corresponding to the strongest emission intensity was determined. Authors suggest that it is the result of concentration quenching owing to the nonradiative energy transfer between luminescent centers increased when the doping concentration rises up. Keeping in mind that the observed concentration of Eu in the materials under investigations was so low, that one cannot be detected by elemental analysis, it's reasonable to assume that concentration quenching is a rare event in these structures. Indeed, the ratio of intensities specific to $^5D_0 \rightarrow {}^7F_2$ and $^5D_0 \rightarrow {}^7F_1$ transitions remains constant for all the measured concentrations of the doped europium. Any broadening or change in the spectrum shape was not observed as well. So, it is reasonable to assume that structural effects related to the maximal level of possible doping specific for perovskite matrix is dominant instead of Eu-Eu electronic interactions. In particular, in [41] it was suggested that solid-solubility limit of europium would be 1…2 mol.% due to large ionic radius difference between Eu^{3+} and Sr^{2+}. In this study, we define that for samples annealed at 1300 °C this limit is lower than 1 mol.%.

In order to check typical for perovskite matrix based materials procedure for decreasing the intrinsic distortion in phosphors containing rare-earth ions by the addition metal ions [45], different amounts of aluminium (1.0 to 10.0 mol.%) were added during the synthetic procedure with a constant effective concentration of Eu equal to 8 mol.%. The results indicate that a monotonic linear increase of the $SrTiO_3$:Eu^{3+}, Al luminescence brightness has been observed with growth of the aluminum concentration. For example, at the Al concentration 10 mol.%, the photoluminescence intensity increases by 2.2 times.

4. Concluding remarks

The $SrTiO_3$:Eu^{3+} red phosphors with different concentrations of accommodated Eu^{3+} ions were prepared using the sol-gel method. The structural analysis showed that the resulting material is a polycrystalline powder consisting of several phases with predominance of $SrTiO_3$ and additional appreciable content of titanium oxide phase in the rutile form. The amount of europium in the phosphors synthesized with less than 8 mol.% of Eu is extremely low; so, the ratio of concentrations Eu/Sr in the final product is essentially low as compared to the original solutions. It was found

that phosphors do not possess magnetic properties, as they contain Eu in a trivalent state. The latter fact confirms the results of luminescence study; the intensity of photoluminescence increases with the Eu concentration up to the maximum level at c.a. 8 mol.%. With increasing the Al concentration up to 10 mol.%, the photoluminescence intensity increases by 2.2 times as well.

Summarizing the results, we can formulate the following conclusions for the samples, the relative concentration of europium in their original solution does not exceed 8 mol.%:

1) the concentration of Eu in phosphors under consideration is lower than the detection limit of the equipment used;
2) the magnetic properties do not appear;
3) luminescent study demonstrates typical luminescence of Eu^{3+} ions in highly symmetrical environment with relatively low distortion of coordination polyhedron.

The collection of the data allows assuming that doped Eu present in a $SrTiO_3$ matrix in very small quantities not correlated with the initial reagents ratio. This suggests that either the europium ions are in the amorphous regions of the material with a large number of structural or crystallite surface defects and do not form a crystalline phase of stable europium compounds with detectable emission or the amount of formed europium compounds is extremely small. The existence of different europium centers in these matrices mentioned for example in Ref. [25]. A possible reason for a small amount of Eu^{3+} in $SrTiO_3$ may be the result of chosen technological conditions including the high temperature ceramic annealing step. However, similar emission is observed in similar phosphors obtained under the high temperature annealing with the temperature exceeding 1200 °C [22, 23, 25] and, at least in [41] mentioned similar low solid-solubility limit of Eu^{3+} in the perovskite matrix. Possible explanation may be related to the low probability process assuming simultaneous exchange substitution of Sr^{2+} and Ti^{4+} sites by Eu^{3+} ions with compensation both electrostatic and spatial distortion within the crystalline structure. However, the ultimate conclusion of this issue requires an additional research.

Acknowledgments

Assistance of Dr. Sc. Miroslav V. Karpets with X-ray measurements is highly appreciated. Authors acknowledge multiple discussions with Dr. Anna N. Morozovska.

References

1. Q.Y. Zhang, X.Y. Huang, Recent progress in quantum cutting phosphors // *Progr. Mater. Sci.* **55**(5), p. 353-427 (2010).
2. V.S. Khomchenko, N.N. Roshchina, L.V. Zavyalova, V.V. Strelchuk, G.S. Svechnikov, N.P. Tatyanenko, V.L. Gromashevskii, O.S. Litvin, E.A. Avramenko, B.A. Snopok, Structure and the emission and piezoelectric properties of MOCVD-grown ZnS, ZnS-ZnO, and ZnO films // *Techn. Phys.* **59**(1), p. 93-101 (2014).
3. D. Naumenko, V. Snitka, B. Snopok, S. Arpiainen, H. Lipsanen, Graphene-enhanced Raman imaging of TiO_2 nanoparticles // *Nanotechnology*, **23**, 465703 (2012).
4. A. Bussmann-Holder, J. Köhler, R.K. Kremer, and J.M. Law, Analogies of structural instabilities in $EuTiO_3$ and $SrTiO_3$ // *Phys. Rev. B*, **83**, 212102 (2011).
5. Z. Guguchia, H. Keller, A. Bussmann-Holder, J. Köhler, R.K. Kremer, The low-temperature magnetic phase diagram of $Eu_xSr_{1-x}TiO_3$ // *Europ. Phys. J. B*, **86**, p. 409 (2013).
6. J Köhler, R Dinnebier, A Bussmann-Holder, Structural instability of $EuTiO_3$ from X-ray powder diffraction, in: *Phase Transitions*. Taylor & Francis, 2012.
7. P.G. Reuvekamp, R.K. Kremer, J. Köhler et al., Spin-lattice coupling induced crossover from negative to positive magnetostriction in $EuTiO_3$ // *Phys. Rev. B*, **90**, 094420 (2014).
8. P.G. Reuvekamp, R.K. Kremer, J. Köhler, and A. Bussmann-Holder, Evidence for the first-order nature of the structural instability in $EuTiO_3$ from thermal expansion measurements // *Phys. Rev. B*, **90**, 104105 (2014).
9. O.M. Marchylo, Y. Nakanishi, H. Kominami, K. Hara, L.V. Zavyalova, V.V. Laguta, S.V. Svechnikov, B.A. Snopok, New high-efficiency red-emitting phosphor produced by the sol–gel method // *Theoretical and Experimental Chemistry*, **50**(1), p. 29-34 (2014).
10. A.N. Morozovska, M.D. Glinchuk, R.K. Behera, B.Y. Zaylichniy, Ch.S. Deo, E.A. Eliseev, Ferroelectricity and ferromagnetism in $EuTiO_3$ nanowires // *Phys. Rev. B*, **84**, 205403 (2011).
11. E.A. Eliseev, M.D. Glinchuk, V.V. Khist, Chan-Woo Lee, Ch.S. Deo, R.K. Behera, and A.N. Morozovska, New multiferroics based on $Eu_xSr_{1-x}TiO_3$ nanotubes and nanowires // *J. Appl. Phys.* **113**, 024107 (2013).
12. A.N. Morozovska, E.A. Eliseev, M.D. Glinchuk, Long-Qing Chen, V. Gopalan, Interfacial polarization and pyroelectricity in antiferrodistortive structures induced by a flexoelectric effect and rotostriction // *Phys. Rev. B*, **85**, 094107 (2012).
13. A.N. Morozovska, E.A. Eliseev, S.V. Kalinin, Long-Qing Chen and V. Gopalan, Surface polar states and pyroelectricity in ferroelastics induced by flexo-roto field // *Appl. Phys. Lett.* **100**, 142902 (2012).

14. A.N. Morozovska, E.A. Eliseev, S.L. Bravina, A.Y. Borisevich, and S.V. Kalinin, Roto-flexoelectric coupling impact on the phase diagrams and pyroelectricity of thin $SrTiO_3$ films // *J. Appl. Phys*. **112**, 064111 (2012).
15. A.N. Morozovska, Yijia Gu, V.V. Khist, M.D. Glinchuk, Long-Qing Chen, V. Gopalan, and E.A. Eliseev, Low-symmetry monoclinic phase stabilized by oxygen octahedra rotations in thin strained $Eu_xSr_{1-x}TiO_3$ films // *Phys. Rev. B*, **87**, 134102 (2013).
16. Koen Binnemans, Interpretation of europium(III) spectra // *Coordination Chemistry Reviews*, **295**, February 2015.
17. C.R. Ronda, Phosphors for lamps and displays: an applicational view // *J. Alloys and Compounds*, **225**, p. 534-538 (1995).
18. A. Kale, N. Shepherd, W. Glass, D. DeVito, M. Davidson, P.H. Holloway, Infrared emission from zinc sulfide: Rare-earth doped thin films // *J. Appl. Phys*. **94**(5), p. 3147-3152 (2003).
19. R.M. Macfarlane, High-resolution laser spectroscopy of rare-earth doped insulators: a personal perspective // *J. Lumin*. **100**, p. 1-20 (2003).
20. Z.R. Hong, C.S. Lee, S.T. Lee, W.L. Li, S.Y. Liu, Efficient red electroluminescence from organic devices using dye-doped rare earth complexes // *J. Appl. Phys. Lett*. **82**(14), p. 2218-2220 (2003).
21. H. Yamamoto, Y. Suda, Luminescence of rare-earth-activated Ga-containing oxides by low-energy electron excitation // *J. Soc. Inf. Disp*. **6**(3), p. 2783-2785 (1998).
22. C.R. García, J. Oliva, M.T. Romero, R. Ochoa-Valiente, and L.A. Garcia Trujillo, Effect of Eu^{3+} concentration on the luminescent properties of $SrTiO_3$ phosphors prepared by pressure-assisted combustion synthesis // *Adv. in Mater. Sci. and Eng.* **2015**, Article ID 291230, 7 p. (2015).
23. Limin Dong, Jian Li, Qin Li, Lianwei Shan, and Zhidong Han, Luminescence performance of yellow phosphor $Sr_xBa_{1-x}TiO_3:Eu^{3+}$, Gd^{3+} for blue chip // *J. Nanomaterials*, **2015**, Article ID 405846, 6 p. (2015).
24. S.P. Feofilov, A.A. Kaplyanskii, A.B. Kulinkin, and R.I. Zakharchenya, Nanocrystalline $SrTiO_3:Eu^{3+}$ and $BaTiO_3:Eu^{3+}$: Fluorescence spectroscopy and optical studies of structural phase transitions // *Phys. Status Solidi* (*c*), **4**, p. 705-710 (2007).
25. R.F. Gonçalves, Rosana de Fátima et al., Crystal growth and photoluminescence of europium-doped strontium titanate prepared by a microwave hydrothermal method // *Ceramics Intern*. **41**(3), p. 3549-3554 (2015).
26. I.K. Battisha, A. Speghini, S. Polizzi, F. Agnoli, M. Bettinelli, Molten chloride synthesis, structural characterisation and luminescence spectroscopy of ultrafine Eu^{3+}-doped $BaTiO_3$ and $SrTiO_3$ // *Mater. Lett.* **57**, Issue 1, p. 183-187 (2002).
27. O.M. Marchylo, L.V. Zavyalova, Y. Nakanishi, H. Kominami, A.E. Belyaev, G.S. Svechnikov, Investigation of luminescent properties inherent to $SrTiO_3:Pr^{3+}$ luminophor with Al impurity // *Semiconductor Physics, Quantum Electronics and Optoelectronics*, **14**(4), p. 461-464 (2011).
28. O.M. Marchylo, Y. Nakanishi, H. Kominami, K. Hara, L.V. Zavyalova, S.V. Svechnikov, B.A. Snopok, Effect of aluminum on the microstructure and photoluminescence of $SrTiO_3:Pr^{3+}$ phosphors prepared by a sol-gel method // *Theoretical and Experimental Chemistry*, **49**(3), p. 147-152 (2013).
29. O.M. Marchylo, Y. Nakanishi, H. Kominami, K. Hara, L.V. Zavyalova, S.V. Svechnikov, B.A. Snopok, Optical converters based on ceramic crystalline phosphor $SrTiO_3:Pr^{3+}$, Al for silicon sensors of ultraviolet radiation // *Theoretical and Experimental Chemistry*, **48**(3), p. 133-138 (2012).
30. A.P. Tomsia and A.M. Glaeser (Ed.), *Ceramic Microstructures: Control at the Atomic Level*. Plenum Press, 1998.
31. I.S. Golovina, V.E. Rodionov, S.A. Khainakov, V.V. Litvinenko, Structure and EPR of low-dimensional powders $KNb_{1-x}Fe_xO_3$ // *Visnyk Kharkivs'koho Natsional'noho universitetu.* Ser. Fizychna "Yadra, chastynky, polia", **1059**, №3(59), p. 96-101 (2013), in Russian.
32. W.S.D. Folly, V.R. Caffarena, R.L. Sommer, J.L. Capitaneo, A.P. Guimaraes, Magnetic properties of $Fe_{90}Zr_7B_3$ ribbons studied by FMR and magnetization // *J. Magn. and Magn. Mater.* **320**, p. e358-e361 (2008).
33. M. Rivoire, G. Suran, Magnetization of thin films with in-plane uniaxial anisotropy studied by microwave absorption // *J. Appl. Phys*. **78**, p. 1899-1905 (1995).
34. I.S. Golovina, S.P. Kolesnik, V. Bryksa et al., Defect driven ferroelectricity and magnetism in nanocrystalline $KTaO_3$ // *Physica B: Condensed Matter*, **407**, p. 614-623 (2012).
35. I.S. Golovina, B.D. Shanina, S.P. Kolesnik et al., Magnetic defects in $KTaO_3$ and $KTaO_3$:Fe nanopowders // *Phys. Status Solidi* (*b*), **249**(11), p. 2263-2271 (2012).
36. M.E. Zvanut, S. Jeddy, E. Towett, G.M. Janowski, C. Brooks, and D. Schlom, An annealing study of an oxygen vacancy related defect in $SrTiO_3$ substrates // *J. Appl. Phys*. **104**, 064122 (2008).
37. I. Bykov, M. Makarova, V. Trepakov, A. Dejneka, L. Yurchenko, A. Jager, and L. Jastrabik, Intrinsic and impurity defects in chromium-doped $SrTiO_3$ nanopowders: EPR and NMR study // *Phys. Status Solidi* (*b*), p. 1-4 (2013).
38. J. Soria, J. Sanz, I. Sobrados, J.M. Coronado, F. Fresno, and M.D. Hernández-Alonso, Magnetic resonance study of the defects influence on the surface characteristics of nanosize anatase // *Catal. Today*, **129**, p. 240 (2007).

39. Photoluminescent properties of $Sr_2SiO_4:Eu^{3+}$ and $Sr_2SiO_4:Eu^{2+}$ phosphors prepared by solid-state reaction method // *J. Rare Earths*, **27**, No. 2, p. 323 (2009).
40. S.B. Meshkova, V.P. Antonovich, S.A. Tarasenko et al., The determination of Eu^{2+} and Eu^{3+} contents in fluorides EuF_{3-x} // *Metody ta ob'ekty khimichnoho analizu*, **4**(2), p. 153-158 (2009), in Ukrainian.
41. Fumito Fujishiro, Tomonori Arakawa, Takuya Hashimoto, Substitution site and photoluminescence spectra of Eu^{3+}-substituted $SrTiO_3$ prepared by Pechini method // *Mater. Lett.* **65**, Issue 12, p. 1819-1821 (2011). http://dx.doi.org/10.1016/j.matlet.2011.03.078.
42. R.F. Gonçalves, A.P. Moura, M.J. Godinho, E. Longo, M.A.C. Machado, D.A. de Castro, M. Siu Li, A.P.A. Marques, Crystal growth and photoluminescence of europium-doped strontium titanate prepared by a microwave hydrothermal method // *Ceramics Intern*. **41**, Issue 3, Part A, April, p. 3549-3554 (2015). http://dx.doi.org/ 10.1016/ j.ceramint.2014.11.018.
43. W.M. Yen, S. Shionoya and H. Yamamoto, *Phosphor Handbook*. CRC press, Boca Raton, 2006, p. 206.
44. C. Jiang, L. Fang, M. Shen, F. Zheng, and X. Wu, Effects of Eu substituting positions and concentrations on luminescent, dielectric, and magnetic properties of $SrTiO_3$ ceramics // *Appl. Phys. Lett.* **94**, Article ID, 071110 (2009).
45. S. Okamoto, H. Kobayashi and H. Yamamoto, Effects of Al addition on photoluminescence properties in rare-earth ion-doped $SrTiO_3$ // *J. Electrochem. Soc*. **147**(6), p. 2389-2393 (2000).